Imaging phonons in a superconductor

M. R. Hauser
Physics Department and Materials Research Laboratory, University of Illinois at Urbana-Champaign, Urbana, Illinois 61801

R. Gaitskell
Center for Particle Astrophysics, University of California at Berkeley, Berkeley, California 94720

J. P. Wolfe
Physics Department and Materials Research Laboratory, University of Illinois at Urbana-Champaign, Urbana, Illinois 61801
(Received 16 April 1999)

We present images of acoustic phonons propagating ballistically through a single crystal of metal: superconducting Nb. Phonons with energy less than twice the superconducting gap have greatly reduced scattering from electrons and can propagate millimeter distances without scattering. We have observed sharp phonon-focusing patterns in niobium. Time and space dependences of the heat pulses provide useful information about the propagation of phonons and quasiparticles in Nb and potentially other superconductors.
[S0163-1829(99)08629-4]

Superconductivity in conventional metals is mediated by phonons that bind electrons into Cooper pairs. Thermally excited phonons with energies greater than twice the superconducting gap can *break* Cooper pairs, creating unpaired electrons, or quasiparticles. Consequently, temperature dependences of the heat capacity and thermal conductivity of metals have provided important confirmations the BCS theory of superconductivity. In such experiments, electrons in the superconducting state interact with phonons in thermal equilibrium at the lattice temperature. Useful information about a superconductor can also be gained by observing the dynamics of *nonequilibrium* phonons, such as those produced in a transient fashion by an electrical current or light pulse.

The potential advantage of using nonequilibrium phonons is that the superconductor can be probed by phonons with selected wave vectors, polarizations and/or frequencies. In this paper we report the observation of ballistic phonon propagation in a single crystal of niobium. Our experiments provide information about the spatial and temporal behavior of nonequilibrium phonons and quasiparticles in this superconductor.

The principal difficulty in observing the propagation of nonequilibrium phonons in a metal is the strong electron-phonon interaction. The existence of the energy gap Δ in a superconductor, however, radically diminishes the scattering rate of phonons whose energy is less than twice the gap. At zero temperature the ideal superconductor becomes completely transparent to phonons with $h\nu < 2\Delta$ because they cannot break Cooper pairs. The mean free path of subgap phonons is limited only by scattering from residual lattice defects and impurities. At nonzero temperature the subgap phonons also scatter from thermally excited quasiparticles.

The transmission of nonequilibrium phonons through a superconductor was clearly demonstrated by Narayanamurti and co-workers,[1] who observed the ballistic propagation of heat pulses through a single crystal of lead at $T < T_c$. They also observed the propagation of nonequilibrium quasiparticles in this crystal. Subsequently, Pannetier and Maneval[2] used phonon spectroscopy to observe the frequency cutoff in the transmission of ballistic phonons in tin, providing a measure of the superconducting gap.

Our experiments employ a high-quality single crystal of niobium, 2 mm thick and 10 mm in diameter.[3] Both flat faces of the sample were oxidized to provide an 1150 Å insulating layer of Nb_2O_5. On one of the faces, we then deposited a 2500 Å film of copper which, when excited by a focused laser beam, acts as a local source of nonequilibrium phonons. A $5 \times 10\ \mu m^2$ granular-Al film was deposited on the opposing face, providing a superconducting bolometer with a transition temperature of 2.1 K. The crystal was immersed in superfluid He, and excitation was provided by a cavity dumped Ar-ion laser ($\lambda = 514$ nm, pulsewidth$=15$ ns).

The angular dependence of the phonon flux transmitted through the crystal at $T = 1.56$ K is shown in the phonon image in Fig. 1(a). Here, transmitted flux is recorded for each spatial position of the laser beam, which is scanned in a raster pattern across the surface of the crystal. The bright features are phonon caustics, similar to those observed previously in semiconductors and insulators.[4] For comparison, a Monte Carlo calculation of the phonon-focusing pattern for Nb is given in Fig. 1(b).[5] The longitudinal (L) mode displays no caustics, and the patterns associated with the slow-transverse (ST) and fast-transverse (FT) modes are identified in the figure. The prominence of the sharp focusing pattern in our crystal implies that a significant fraction of the phonons are traveling ballistically across the 2-mm thick sample, i.e., without scattering.

Figure 2(a) shows the corresponding heat pulses for three different excitation energies. The propagation direction for the phonons, determined by the relative positions of the laser spot and the detector, is approximately 20° from [110], corresponding to the white dot in Fig. 1(a). The predicted ballistic time-of-flights for the L, FT, and ST modes are shown by arrows and correspond to the leading edges of the observed pulses. Superimposed on the ballistic pulses is a

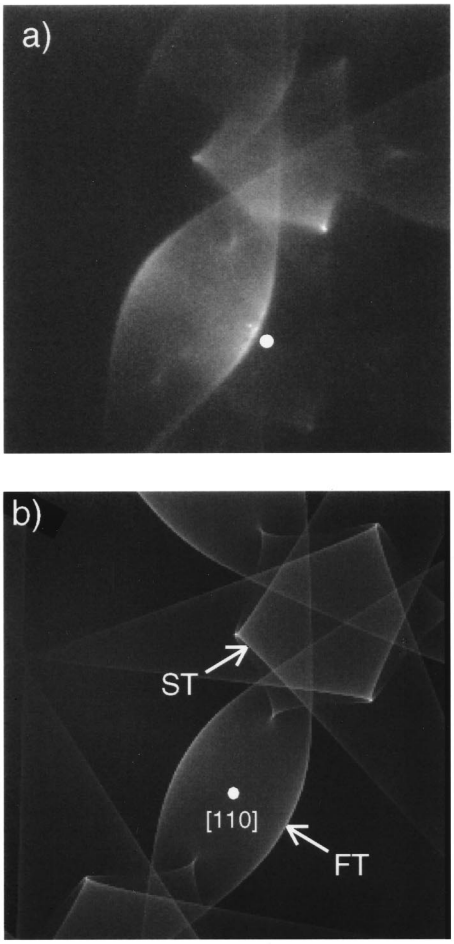

FIG. 1. (a) Phonon image at low excitation power (1.5 nJ/pulse) showing caustics in phonon flux. The twofold symmetric [110] and threefold symmetric [111] structures are evident. The white dot shows the location of the time traces in Fig. 2(a). (b) Calculated phonon-focusing pattern for Nb.

broad tail extending beyond 4000 ns and becoming more pronounced as the excitation energy is increased.

The intensity of the L pulse as a function of the incident energy is plotted as the dots in Fig. 2(b). At low excitation levels the phonon flux increases roughly linearly with the power, but a pronounced sublinear behavior is observed at high power. To understand this behavior, we consider the source of phonons from the heater film to be described by a Planckian distribution with a temperature T_h. As the heater temperature is raised, an increasing fraction of phonons have energies greater than twice the superconducting gap in niobium, $h\nu > 2\Delta = 3.03\,\mathrm{meV}$. The total energy carried by phonons that are unable to break Cooper pairs is given by

$$E_{\mathrm{subgap}} = \int_0^{2\Delta/h} d\nu h\nu D(\nu) n(\nu)$$

$$= \int_0^{2\Delta/h} d\nu \frac{6h\nu^3}{v^3} \frac{1}{e^{h\nu/k_B T} - 1}, \qquad (1)$$

where v is the average phase velocity of the phonons, $D(\nu)$ is the phonon density of states, and $n(\nu)$ is the phonon occupation number. At temperatures such that $2\Delta \ll k_B T_h$, the value of the integral is proportional to the heater temperature, giving $E_{\mathrm{subgap}} \propto T_h$.

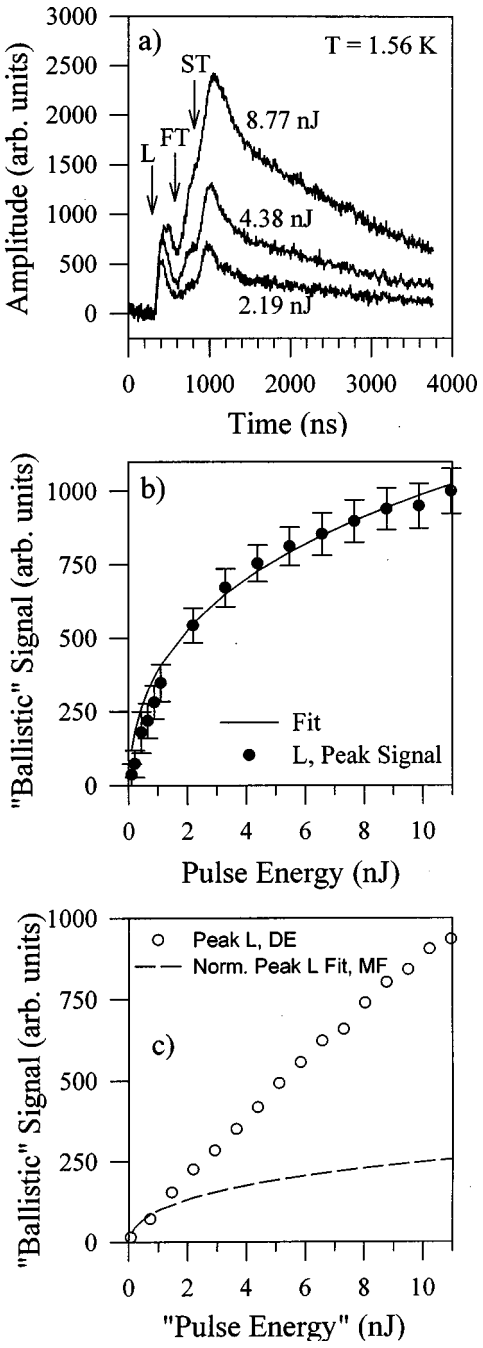

FIG. 2. (a) Heat pulses for three excitation energies. Propagation direction is indicated by the white dot in Fig. 1(a). Calculated ballistic arrival times for L, FT, and ST phonons are indicated by the arrows. (b) Peak intensity of the L mode as a function of excitation energy for the case with a Cu film on the excitation surface. (c) Peak intensity of the L mode vs excitation energy for direct excitation of the Nb surface. The dashed line is the theoretical curve from (b) with the scale adjusted to normalize the slopes of the metal-film (MF) and direct excite (DE) data at low powers.

The local temperature of the heated spot can be estimated from the Stefan-Boltzmann law modified for phonons,[6] $P/A = \sigma(T_h^4 - T^4)$, where P is the instantaneous radiated power, A is the surface area of the heated film, T is the lattice

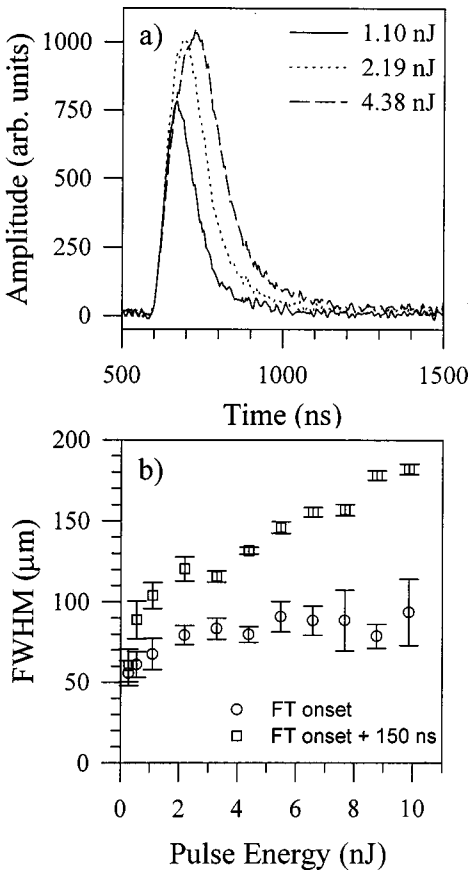

FIG. 3. (a) Spatially filtered phonon signals with metal-film excitation. The duration of the phonon source increases with increasing excitation energy, as does the time of the peak signal. (b) Phonon source size (FWHM of the FT caustic) vs power for two sampling times.

temperature, and σ is the effective emissivity of the film. This equation implies that for $T_h \gg T$, the heater temperature increases as $P^{1/4}$. For a pulse length Δt, $P = E_{\text{pulse}}/\Delta t$, so at high excitation energies we predict a sublinear dependence of the ballistic phonon flux, $E_{\text{subgap}} \propto E_{\text{pulse}}^{1/4}$.

A fit of Eq. (1) to the data is plotted as the solid line in Fig. 2(b). Here it is assumed that the heater temperature is given by $T_h = (E_{\text{pulse}}/A\sigma\Delta t)^{1/4}$. Assuming a pulse width $\Delta t = 15\,\text{ns}$ and an irradiated spot with a full width at half maximum (FWHM) of 20 μm, the only adjustable parameter is the emissivity of the metal film into the Nb. The fitted emissivity turns out to be $\sigma = 707\,\text{Wm}^{-2}\,\text{K}^{-4}$, which is within 12% of the value expected from the acoustic-mismatch model applied to the materials at hand. The reasonable agreement between experiment and theory, shown in Fig. 2(b), confirms the idea of a gap-controlled ballistic phonon transmission.

A remarkably different result is obtained by optically exciting the Nb crystal directly, rather than exciting a copper film on the surface. While this situation is considerably more difficult to describe quantitatively, one expects that the hot carriers created by the photons relax by the emission of high energy phonons and the creation of quasiparticles. This process apparently does not lead to a localized Planckian source, as the data in Fig. 2(c) indicate. In this case, a linear dependence is observed between the detected phonon flux and the incident optical energy, implying that the frequency dependence of the emitted phonons does not change significantly with excitation power.

Returning to the metal-film excitation of the Nb crystal, we consider the characteristics of the phonon source. The temporal profile of the source can be estimated by spatially filtering the phonon signal.[7] The ''off-caustic'' signal is subtracted from the ''on-caustic'' signal, thereby removing the effect of phonons scattered in the bulk, whose flux varies only slowly with angle. Spatially filtered signals are shown in Fig. 3(a) for three different excitation levels. The source lifetime (the width of the pulse) is seen to increase markedly with excitation energy, as does the time of the peak signal.

The *size* of the source can be estimated from the width of the caustics in the phonon images, since these structures would be infinitely sharp for a point source. The width of the FT caustic near [110] is plotted as a function of excitation energy in Fig. 3(b). The sharpness of the caustic decreases with time and with excitation energy, as indicated by the data at two sampling times. This implies that the ballistic-phonon *source size* increases with incident energy and time.

The power dependence of the source size is dramatically demonstrated in the phonon images of Fig. 4. The phonon image for an input energy of 5.5 nJ [Fig. 4(a)] displays

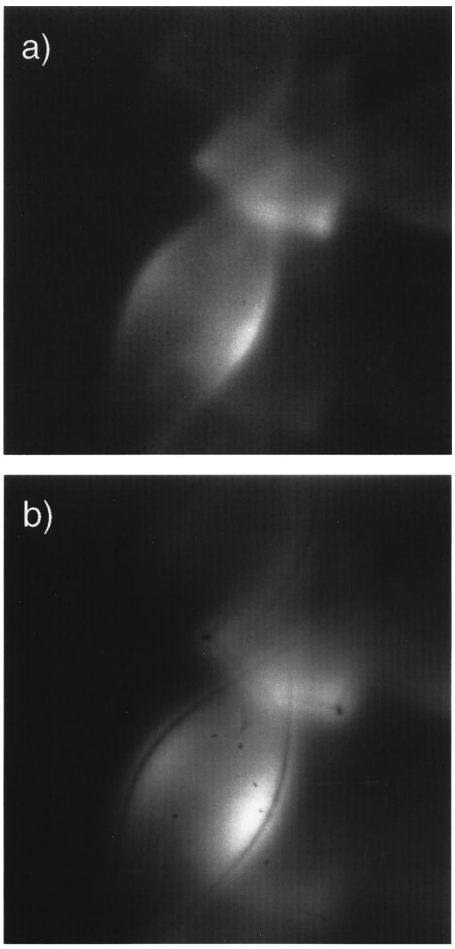

FIG. 4. Phonon images for (a) 5.5 nJ incident pulse energy, showing a broadening of the caustics compared to Figs. 1(a) and 1(b) 16 nJ incident pulse energy, showing broad caustics produced by the pulse and sharp ''dark caustics'' from the subtracted low-power signal.

broader caustics than at lower power [Fig. 1(a)]. The caustics are even broader in Fig. 4(b), but an additional structure is superimposed—the ''dark caustics.'' This image is obtained by exciting with a low level of continuous laser light in addition to the 10-ns pulses. The boxcar integrator subtracts the pattern due to the low-level source from that of the high-level pulsed source, producing very sharp dark caustics on top of broader bright caustics.[8]

Why does the phonon source size increase with time and pulse energy? One source of ballistic phonons is from the thermalization of photoexcited electrons, which is quite localized. However, thermalized quasiparticles also produce nonequilibrium phonons as they recombine into Cooper pairs. As the quasiparticles diffuse away from the excitation point, they provide a phonon source of increasing size. This process is qualitatively consistent with observations of both the temporal and spatial behavior of the source.

If the quasiparticles were acting as scattering centers for ballistic phonons, trapping the phonons in a small region at early times, then the size of the trapping region (i.e., the phonon source size) would initially increase in time as the quasiparticles diffused away from the source. This agrees qualitatively with measurements of the caustic-size vs time [e.g., Fig. 3(b)]. Phonon generation by recombination of the nonequilibrium quasiparticles could also give rise to an expanding phonon source. The idea that the quasiparticles are acting as a significant source of nonequilibrium phonons can explain the long tails in Fig. 2(a). While the heights of the phonon peaks increase sublinearly with increasing excitation energy, the total detected flux, obtained by integrating an entire time trace, increases nearly *linearly* with excitation energy. This observation implies that the nonequilibrium quasiparticles are recombining and generating subgap phonons which are then detected by the bolometer.

In conclusion, we have obtained the first phonon images in a metal thanks to the remarkable effect of the superconducting state to decouple subgap phonons from the electronic system.[1,2] The presence of sharp focusing structures makes it possible to deconvolve scattered phonons from ballistic phonons with well defined wave vectors. Thus imaging allows the examination of the spatial and temporal development of the nonequilibrium excitations created by a heat pulse. In Nb an expanding source of ballistic phonons is observed which, we believe, gauges the diffusing cloud of nonequilibrium quasiparticles. More generally, phonon imaging may provide an angle-sensitive probe of the anisotropy of the superconducting state in more exotic superconductors.

This work was supported in part by the National Science Foundation by the Materials Research Laboratory Grant No. NSF DMR 898-20538 and by the Department of Energy MRL Grant No. DEAC02-76ER01198.

[1] V. Narayanamurti, R. C. Dynes, P. Hu, H. Smith, and W. F. Brinkman, Phys. Rev. B **18**, 6041 (1978); P. Hu, R. C. Dynes, V. Narayanamurti, H. Smith, and W. F. Brinkman, Phys. Rev. Lett. **38**, 361 (1977).

[2] B. Pannetier, D. Huet, J. Buechner, and J. P. Maneval, Phys. Rev. Lett. **39**, 646 (1977); B. Pannetier and J. P. Maneval, Phys. Rev. B **23**, 85 (1981).

[3] The crystal was grown by Klaus Schulze at the Max-Planck Institute fur Mattallforschung in Stuttgart. Our sample was spark cut from a 10-mm diameter boule and had a crystal orientation of [0.807, 0.559, 0.191]. The residual resistance ratio was $\sim 10^4$. Before oxidation, the sample was etched in a solution of 1 HF: 2 HNO_3 for 0.5 to 5 min, then rinsed in deionized water.

[4] G. A. Northrop and J. P. Wolfe, in *Nonequilibrium Phonon Dynamics*, edited by W. E. Bron (Plenum, New York, 1985); J. P. Wolfe, *Imaging Phonons* (Cambridge University Press, Cambridge, 1998).

[5] Elastic constants were taken from G. Simmons and H. Wang, *Single Crystal Elastic Constants and Calculated Aggregate Properties Handbook* (M.I.T. Press, Cambridge, MA, 1971).

[6] O. Weis, in *Nonequilibrium Phonons in Non-Metallic Crystals*, edited by W. Eisenmenger and A. A. Kaplyanskii (Elsevier, Amsterdam, 1986), p. 1; O. Weis, Z. Angew. Phys. **26**, 325 (1969).

[7] M. Greenstein, M. A. Tamor, and J. P. Wolfe, Phys. Rev. B **26**, 5604 (1982).

[8] M. R. Hauser, Ph.D. thesis, University of Illinois at Urbana-Champaign, 1995.